

Measurements and simulations of the BLM response to a radiation field inside the CERF target area

E. Lebbos, M. Brugger, B. Dehning, E. Effinger, A. Ferrari, D. Kramer,
A. Nordt, K. Roed, S. Roesler, M. Sapinski, V. Vlachoudis

Abstract

The CERN-EU high-energy reference field (CERF) facility is installed in one of the secondary beam lines (H6) of the Super Proton Synchrotron (SPS), in the North Experimental Area at CERN. This facility is used as a reference for testing, inter-comparing and calibrating passive and active instruments. In May 2009, the SPS provided a mixed hadron beam (protons, pions and kaons) during a few days, in order to perform several measurements with different devices such as the Radiation Protection Monitor used for residual dose rates due to Induced Radioactivity in the LHC (PMI), the Secondary Emission Monitor used for high beam losses (SEM), the Radiation Monitor for electronics (RadMon), and the Beam Loss Monitor for the LHC (BLM). This report focuses on the measurements of the BLM response during this year's operation at CERF. The measurements evaluate the sensitivity of the BLM signal to the particle energy spectrum, with special attention to the contribution coming from thermal neutrons. For this purpose, measurements are performed at various calibrated positions with different fields, as well as by using a Cd layer which is wrapped around the detector. The fields the BLM detector is exposed to are representative for the LHC and range from fields typical to the LHC tunnel, up to radiation fields encountered in shielded areas close to the LHC tunnel. For all configurations, detailed FLUKA simulations were performed to benchmark in detail the reproducibility of the BLM signal. In addition, to evaluate the BLM response in terms of energy deposition and particles spectra, dedicated calibration calculations were performed to provide energy and particle dependent response functions of the BLM detector. This allowed calculating the contribution of the main particles to the BLM signal and their respective energy range. This successful benchmark shows not only the high accuracy which can be achieved when performing radiation field estimates of LHC like spectra with the FLUKA Monte-Carlo code, but also clarifies the possible issue of low-energy neutrons seen by the BLM detector.

1. Introduction

The CERN-EU High Energy Reference Radiation Field (CERF) [1] facility is installed in one of the secondary beam lines (H6) from the Super Proton Synchrotron (SPS), in the North Experimental Area at CERN. A positively charged hadron beam with a momentum of 120 GeV/c is impinging on a copper target of 7 cm in diameter and 50 cm in length. The composition of the incident beam is a combination of pions, protons and kaons.

This facility, built at CERN in the earlier 90's [1], provides a reference for testing, inter-comparing and calibrating passive and active instruments. The Beam Loss Monitor (BLM) is used at the LHC to detect beam losses in the dispersion suppressor, arcs, inner triplets as well as the beam-cleaning insertions. Its use will be important to protect the LHC elements from damage and superconducting magnets from quench. The knowledge of its signal and its sensitivity in a well known radiation field is crucial, and the CERF facility provides good conditions to test such a device. In fact the CERF source spectra at the respective BLM locations are comparable with those at the LHC: they are dominated by low-energy neutrons at the location upstream of the target, and dominated by high-energy particles downstream of the target. This way the upstream and lateral measurement positions provide representative spectra for the BLM locations at the side of superconducting magnets, those slightly further downstream to those next to the warm magnets, as well as the most downstream ones will then correspond to the BLMs put close to collimators [2]. In particular, the main goal of this year's measurement was to evaluate the BLM sensitivity as a function of its orientation, depending on whether the cables are in the upstream position or in the downstream position. A second goal was to measure the sensitivity to low-energy neutrons of the BLM. This was done by cutting the thermal neutron contribution with a Cd layer put all around the BLM.

The experimental measurements were performed between the 8th and the 18th of May 2009. The first two days were devoted to alignment tests and detectors positioning around the target. Then, it was decided to wrap the BLM with a thin layer of Cd in order to evaluate the sensitivity of the BLM signal to low-energy neutrons. This report presents in a first part the experimental set-up as well as the BLM measurements results.

The FLUKA [3] [4] code was used to simulate the CERF experimental conditions and compute the BLM response in terms of energy deposition and particle energies spectra they are exposed to. Additional calculations were performed to evaluate the various contributions, the particle type and the energy following the position of the monitor around the target. The simulation results are shown in the second part.

2. Experimental set-up and measurements

The experiments took place in the CERF test area along the H6-beam line, housed in building EHN1 (SPS north experimental hall). The H6-beam line is providing a secondary beam produced by the primary SPS beam hitting a Be-target T4. The H6-beam consists of different percentages of protons, pions and kaons depending on the momentum that can be tuned between 10 GeV/c

and 205 GeV/c [5]. The momentum of the beam was equal to 120 GeV/c with a particle composition of 60.7% pions, 34.8% protons and 4.5% kaons.

An overall picture of the CERF facility is presented in Figure 1 [6].

The intensity of the SPS secondary beam to the CERF facility is monitored by a Precision Ionization Chamber (PIC). The PIC-counter is installed about 405 m downstream of the T4 production target. It is an open air Ionization Chamber with a cylindrical shape. The charge produced by ionization of the beam in this volume is collected at a capacitor. Whenever this charge reaches a certain value, the capacitor is discharged and one count is scored which represents a given number of beam particles [5]. The PIC serves to normalize the experimental data to the number of particles in the H6 beam. One PIC count corresponds to $22116 \text{ particles} \pm 10\%$ [5].

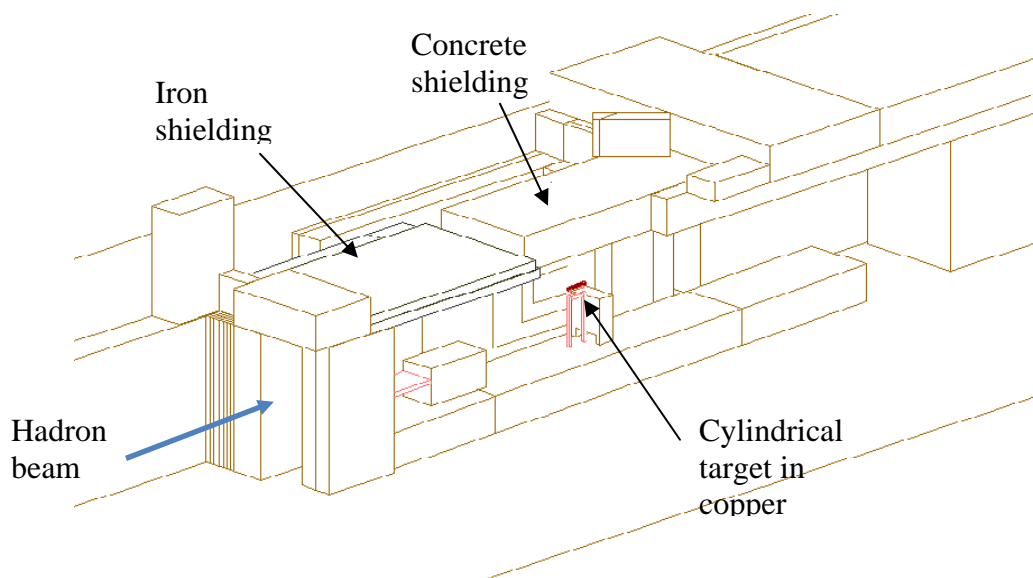


Figure 1: Layout of the CERF facility in the North Experimental Hall as modeled in FLUKA. The side shielding in front is removed to show the inside of the target area [6].

In order to study the response of BLMs to a mixed radiation field, six positions were defined around the CERF target. It has been decided to keep the same measurement positions for this year's tests as those used for a PMI-benchmark in the past [6]. These positions are shown in Figure 2 and more details are presented in Table 1. The coordinate parallel to the wall is the Z coordinate, the coordinate perpendicular to the wall is the Y coordinate, and the vertical axis is the X axis. The target and the beam are not aligned with the Z axis; they form an angle of 2.29° .

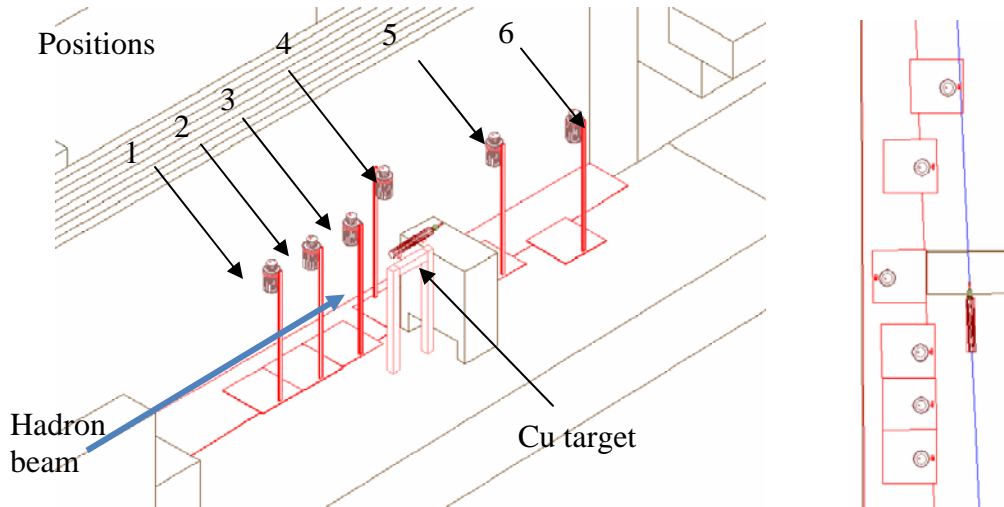


Figure 2: Layout of the test area showing the 6 detector positions around the target (concrete wall in front partially removed) [6].

	Coordinate parallel to wall [cm]	Coordinate perpendicular to wall [cm]		Coordinate parallel to wall [cm]	Coordinate perpendicular to wall [cm]
Pos 1	-100.5	-49.5	Pos 4	70.5	-80.3
Pos 2	-50.5	-49.5	Pos 5	176	-47.5
Pos 3	0.0	-50.0	Pos 6	250	-22.5

Table 1: Coordinates of the centre of the active detector volumes as seen from the beam impact point on the target. The height of all centers was set at beam level [6].

A previous study [2] expected that the CERF source spectra at the respective BLM locations are comparable with those at the LHC: the spectra at positions 1 and 2 are similar to those for the BLM located close to the superconducting magnets, positions 3 and 4 for the BLM located around the warm magnets, and positions 5 and 6 for locations close to collimators. Therefore the main advantage of the CERF facility consists in a large radiation field variety depending on the position chosen around the target, as illustrated in Figure 3 which shows the neutron spectra at the 6 BLM positions around the target as calculated by FLUKA, as well as in the LHC tunnel at point 1. In this plot, one can clearly observe the difference between the thermal neutrons produced at the upstream positions of the target (positions 1 and 2) and the downstream positions 5 and 6, up to a factor 2. The high energy neutrons above 1 GeV are present mostly in the downstream positions, and the neutrons around few MeV are more dominant at position 3, where the detector is placed at 90° with respect to the beam direction.

In order to put in evidence the large radiation field profile, Figure 4 shows the high energy hadron fluence (above 20 MeV) around the CERF target as calculated by FLUKA.

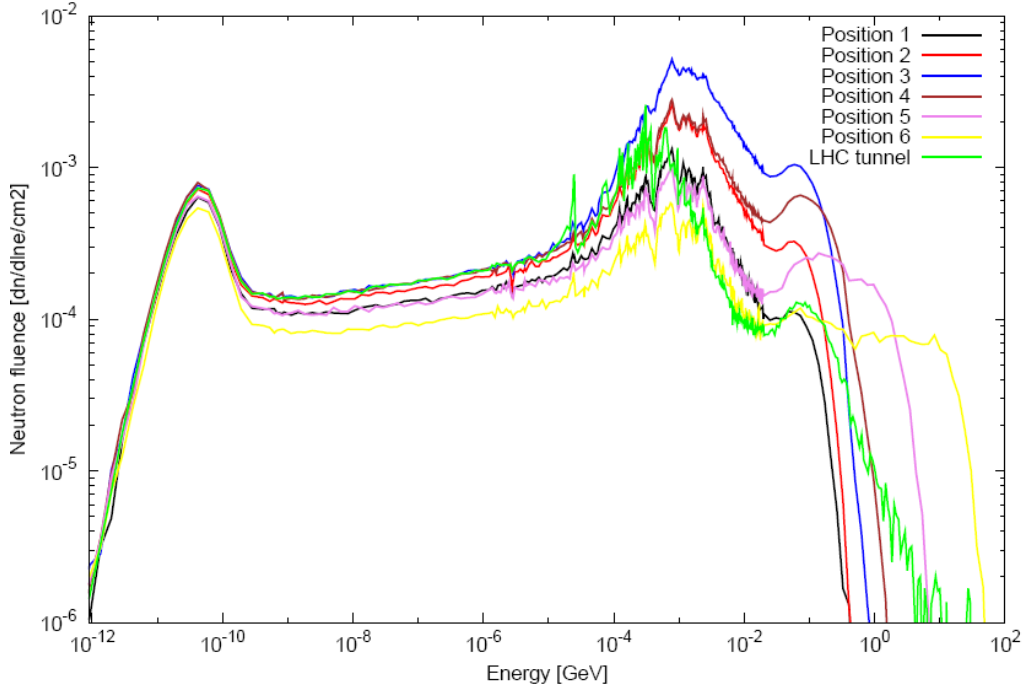


Figure 3: Neutron energy spectra per primary particle entering the CERF BLM active volumes, as calculated by FLUKA. A comparison with the neutron spectra as calculated by FLUKA in the LHC tunnel (IR1 – Q6) is shown.

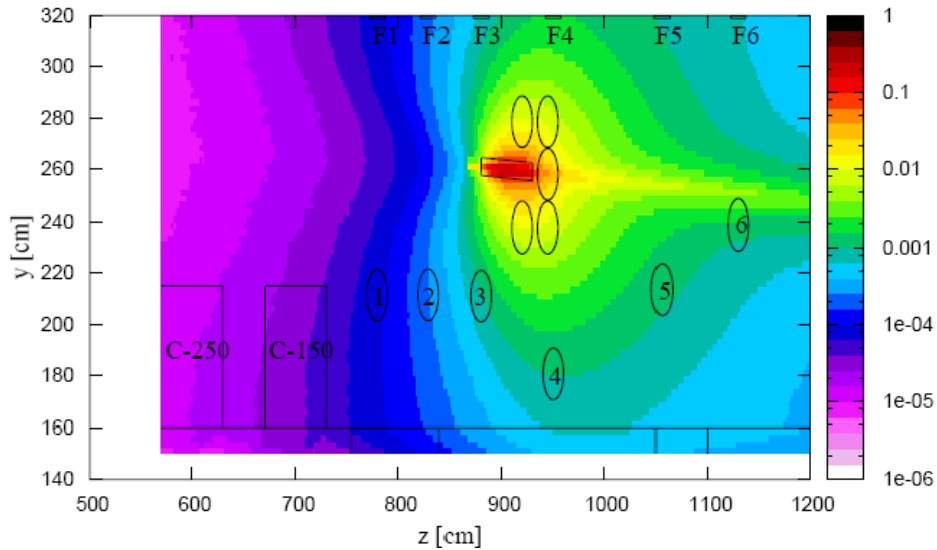


Figure 4: High energy hadron (>20MeV) fluence per primary particle around the CERF target. The six positions of the monitors are put in evidence by numbers surrounded by black circles.

Figures 5 and 6 show the spectra provided by the CERF facility for protons, pions, muons, photons, electrons and positrons at positions 1 and 6 as calculated with FLUKA. Whereas low- and medium-energy neutrons (see also Figure 3) and photons dominate at position 1, the cascade is clearly shifted to high-energies at position 6.

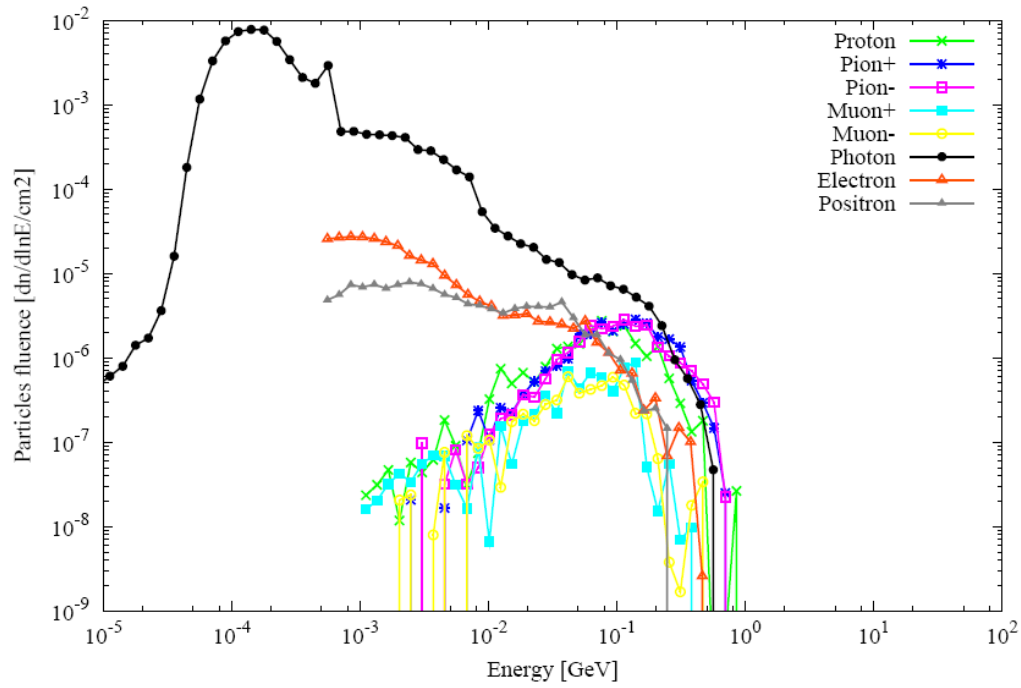


Figure 5: Particle energy spectra entering the CERF BLM detector at position 1.

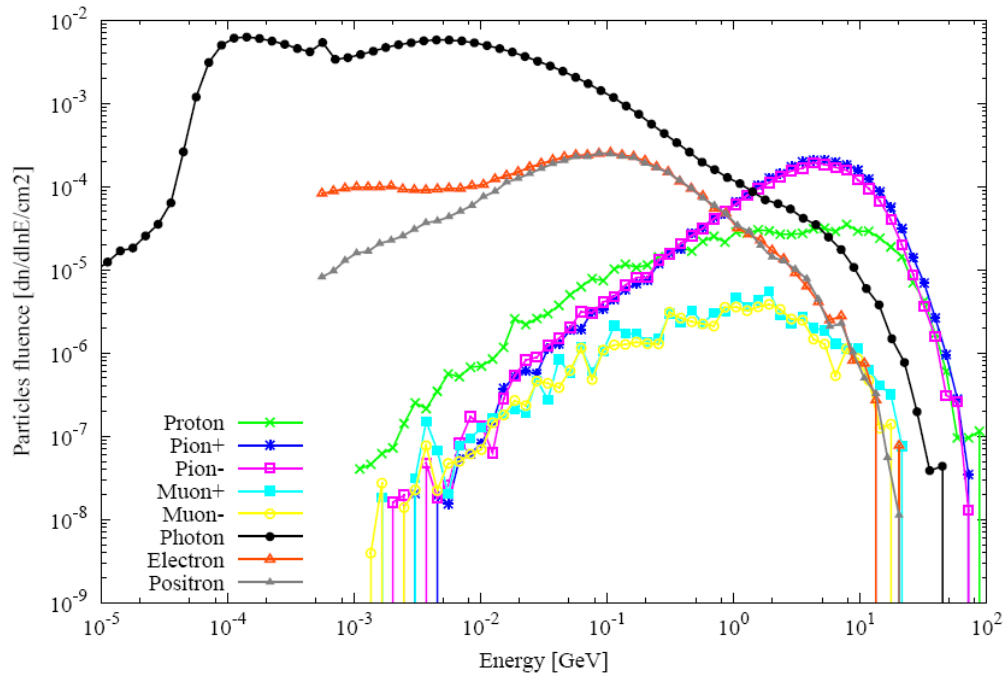


Figure 6: Particle energy spectra entering the CERF BLM detector at position 6.

In terms of particles contribution, Table 2 gives the respective contribution of each particle in relation to the total particles fluence as calculated by FLUKA at each position. For the neutrons, the contribution has been divided into 3 parts: the thermal neutron contribution below 0.5 eV, the

neutrons between 0.5 eV and 100 keV, and the neutrons above 100 keV (see Figure 3). The choice of energy cuts is motivated by the neutron capture cross section on nitrogen as illustrated in Figure 7 showing the neutron capture cross-section in the energy range from below 1eV and up to 10MeV. The contribution from thermal neutron is not negligible (cf. Figure 3) and as shown in Figure 7, the production of a recoil proton from the neutron capture cross section on nitrogen ($^{14}\text{N}(n,p)^{14}\text{C}$) will create ionization and therefore a signal from the BLM.

Position	Particles contribution [%]											
	n				p	π^+	π^-	μ^+	μ^-	γ	e-	e+
	< 0.5 eV	0.5eV<n<100keV	>100keV	Total								
1	5.96	9.52	13.92	29.34	0.03	0.03	0.04	0.01	0.01	70.09	0.32	0.13
2	2.91	5.04	11.89	19.85	0.04	0.06	0.06	0.01	0.01	79.42	0.38	0.17
3	0.79	1.62	7.79	10.20	0.09	0.08	0.08	0.01	0.01	88.75	0.52	0.26
4	1.05	1.97	6.15	9.16	0.21	0.15	0.15	0.01	0.01	88.52	1.20	0.59
5	1.51	2.18	4.30	7.99	0.50	0.67	0.67	0.03	0.03	84.25	3.94	1.91
6	0.96	1.19	2.33	4.48	0.45	1.03	0.95	0.03	0.02	81.85	7.13	4.06

Table 2: Main contributing particles for the respective radiation field at CERF.

Table 2 shows an important contribution of neutrons and photons at position 1, whereas the photons and electrons are more dominant at position 6.

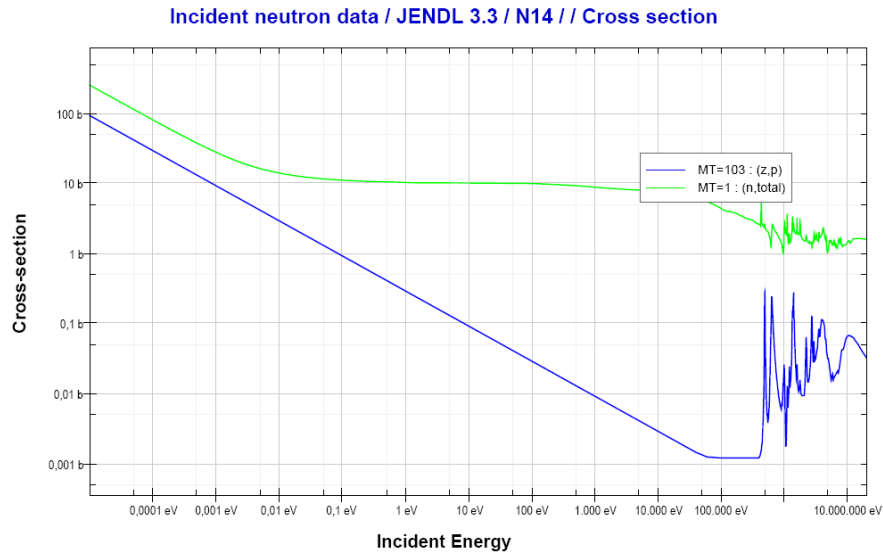


Figure 7: Neutron capture (JENDL) cross section as a function of incident neutron energy [7].

Each measurement was done separately, one position after the other, because only one BLM readout channel was available. Figure 8 shows one BLM mounted vertical and the other horizontal, both installed on the same support. For certain positions, three orientations of the BLM were used. One orientation corresponds to the BLM horizontally oriented, the cables being put downstream according to the beam direction. Another orientation is the BLM at the horizontal but the cables in the upstream direction. And a last orientation is the vertical one with the cables down below. The goal is to see a possible difference in the BLM response depending on the BLM orientation and the orientation of the cables and within the different spectra. The

various positions are representative of the LHC: BLM chambers placed alongside the warm and cold magnets (horizontal orientations) and the BLMs placed downstream of collimators (vertical orientation). In addition, to evaluate the contribution of the low-energy neutron fluence to the BLM signal, for one series of measurements a layer of Cd was wrapped around the BLM (see Figure 8 b).

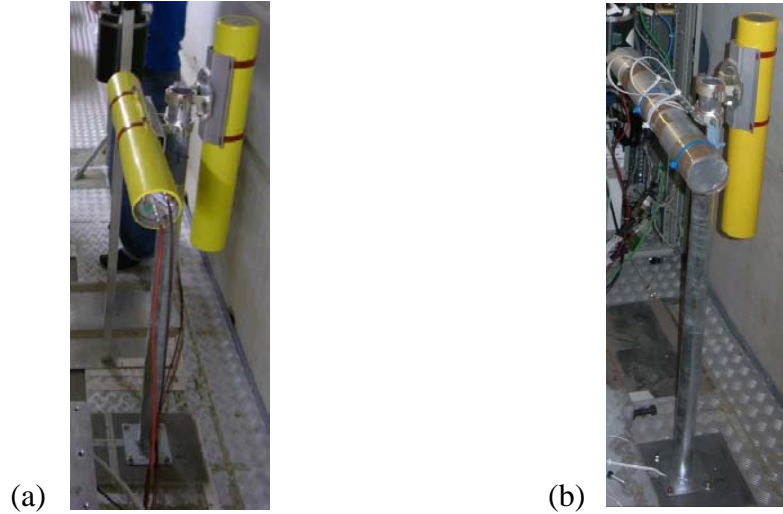


Figure 8: (a) Picture of the horizontally oriented BLM and the vertically oriented BLM, both fixed on the same support. (b) Picture of the BLM wrapped with Cd (the one horizontally oriented).

Because of time constraints and since the measurements with Cd are more relevant at the upstream positions of the target where the thermal neutrons are more dominant, the measurements with Cd were performed only at positions 1 to 3 whereas the measurements without Cd were performed at all positions. Table 3 gives a summary of the different configurations used for the measurements.

BLM configuration		POSITION					
		1	2	3	4	5	6
BLM without Cd	Horizontal cables downstream	x	x	x	x	x	
	Horizontal cables upstream	x	x	x	x	x	x
	Vertical cables down				x	x	x
BLM with Cd	Horizontal cables downstream						
	Horizontal cables upstream	x	x	x			
	Vertical cables down						

Table 3: The cross indicates the BLM measurements performed at CERF in May 2009.

The measurements took around 15 minutes for each position and each orientation. For every irradiation ten beam pulses were used taking note of the BLM signal and the respective beam intensity (PIC). The electronics used to measure charge was Keithley 6517A Electrometer, which has about 10 fC accuracy. The results are summarized in Tables 4, 5 and 6 as average over the recorded beam pulses together with the corresponding uncertainties. These uncertainties calculated by the standard deviation method are higher by at least 2 orders of magnitude than the

accuracy of the Electrometer for all positions. The results are presented in nC and normalized by the number of PIC counts. As mentioned previously, one PIC count corresponds to 22116 particles \pm 10% [5].

First of all, in order to test the sensitivity of the BLM following its orientation, a first series of measurements were performed for the six positions as shown in Table 4. The observed ratio shows only a small difference below 10% as observed in the simulations (see the following paragraph), except for position 1 where low-energy neutrons are more dominant. However it has to be noted that the measurement performed at position 1 with the BLM cables in the downstream direction was not updated because of time constraint, and a serious doubt about the positioning error is considered. It is also the case for the position 3 (cables downstream). No comparison could be done at position 6 because the BLM was installed only with the cables in the upstream direction.

Measurements [nC/PIC] - BLM horizontal without Cd						
	Cables downstream	Error [%]	Cables upstream	Error [%]	Ratio up./down.	Error [%]
Position 1	3.89E-05	1.3	5.18E-05	0.6	1.33	1.9
Position 2	1.33E-04	0.4	1.35E-04	0.2	1.02	0.6
Position 3	5.97E-04	2.3	6.62E-04	0.1	1.11	2.4
Position 4	9.41E-04	0.6	9.07E-04	0.8	0.96	1.4
Position 5	1.17E-03	0.1	1.14E-03	0.1	0.97	0.2
Position 6			2.64E-03	0.6		

Table 4: BLM signal as measured at CERF. Both orientations of the BLM are compared.

A second series of measurements was performed using 1 mm of Cd wrapped around the BLM. The goal was to discriminate the thermal neutron contribution to the BLM signal. Therefore, the BLM was put only at positions 1 to 3 for these measurements because these positions are more dominated by low-energy neutrons. The results were compared with the case without Cd and are shown in Table 5. Almost no difference is observed between the two cases (3% to 4%), possibly meaning that the loss of the contribution to the BLM signal from the thermal neutrons may be compensated by the photons coming from the neutron capture on the Cd. Therefore, in addition to the analysis of the low-energy neutron contribution it has been decided to perform additional MC-calculations to evaluate the BLM signal as a function of incoming particle spectra. The simulations considered both a BLM without Cd as well as a BLM surrounded by 1 mm of Cd.

Measurements [nC/PIC] - BLM horizontal cables upstream						
	Without Cd	Error [%]	With Cd	Error [%]	Ratio Cd /no Cd	Error [%]
Position 1	5.18E-05	0.6	4.96E-05	0.5	0.96	1.1
Position 2	1.35E-04	0.2	1.29E-04	0.1	0.96	0.3
Position 3	6.62E-04	0.1	6.85E-04	0.2	1.03	0.3

Table 5: BLM signal as measured at CERF at 3 positions. Both cases are compared: BLM without Cd and BLM with Cd.

Finally, the measurements at positions 4 to 6 were performed with the BLM vertically oriented and with the cables oriented below. In these positions the BLM-signal is more dominated by high-energy particles and corresponds in terms of radiation field to the location of BLMs close to the collimators in the LHC tunnel. The measurement results are shown in Table 6.

Measurements [nC/PIC] - BLM without Cd						
	Vertical	Error [%]	Horizontal	Error [%]	Ratio hor./vert.	Error [%]
Position 4	9.35E-04	0.6	9.07E-04	0.8	0.97	1.4
Position 5	1.22E-03	0.7	1.14E-03	0.1	0.93	0.8
Position 6	1.81E-03	1.2	2.64E-03	0.6	1.46	1.8

Table 6: BLM signal as measured at CERF at 3 positions. Both cases are compared: BLM vertically oriented and BLM horizontally oriented.

During the measurements the maximum beam intensity on the target corresponded to about 4000PIC (about 108 particles on target). The beam extraction from the SPS was performed during about 4 seconds (flat top with constant intensity), thus the charge production and respective current reach a maximum of about 50 μ A, still well in the linearity range of the BLM chamber (see [9], e.g., Figure 5.3 and 6.11).

3. FLUKA simulations

The FLUKA Monte-Carlo code was used to simulate the experimental conditions, taking into account a representative geometry of the CERF target area with the shielding around (see Figure 1 and Table 7) as already used in previous calculations [2, 6], and a detailed BLM model as shown in Figures 9 and 10.

Table 7 describes the materials composition as defined in the FLUKA simulation.

MATERIAL	DESCRIPTION	DENSITY [g/cm ³]
Concrete	O (48.204%), Si (16.175%), Ca (23.929%), Al (2.113%), Na (0.446%), Fe (1.263%), H (0.561%), C (4.377%), Mg (1.512%), S (0.414%), K (0.833%), Ti (0.173%)	2.4
Steel	Fe (86.32%), Cr (11.14%), Ni (2.53%)	7.7

Table 7: Materials composition in mass fractions as defined in FLUKA.

The implemented BLM model [8] has a total length of 59.9 cm and a diameter of 8.9 cm, consisting of various regions with a central part of parallel plates which enclose the sensitive volume of the detector.



Figure 9: Inside view of a Beam Loss Monitor showing the electronic part at left and all the electrodes put in parallel at right.

For the simulation of each BLM position around the target, 5 CPUs were used for a total number of 100000 incident particles, corresponding to about 4 days of simulation for each configuration. A source routine was used defining the exact composition of the CERF hadron beam. Furthermore, three BLM prototypes are defined in the FLUKA input file and automatically inserted at the respective measurement location around the target by applying the correct rotations and transformations (FLUKA “lattice” operations). Due to the placement of the chambers during the measurement, the coordinates of the positions as defined in the Table 1 correspond to the centre of the BLM sensitive volume and not the centre of the detector itself. The BLM prototypes are illustrated in Figure 10. The reason of simulating a gap at the extremity of the BLM for the third prototype is to verify a possible difference in the particle spectra because of the cable passages.

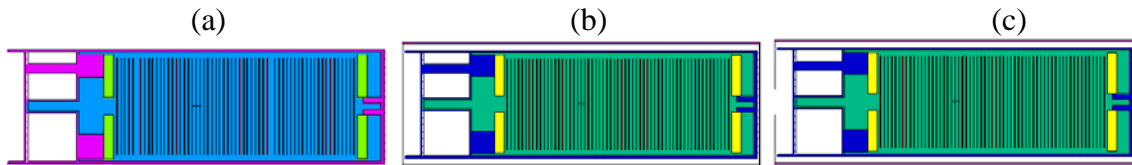


Figure 10: (a) FLUKA model of the BLM prototype number 1 without Cd.
 (b) FLUKA model of the BLM prototype number 2 surrounded by 1 mm of Cd.
 (c) FLUKA model of the BLM prototype number 3 surrounded by 1 mm of Cd and with a small aperture of 2 cm of diameter for cable passages in the electronic part at left.

To reduce the time of the simulation the BLMs were put in all positions for a same calculation. A possible alteration of the particle field due to the presence of numerous BLM chambers was checked through an additional calculation and is shown to be negligible as illustrated for example in Figure 11 where it is shown that no significant difference was observed in terms of neutron spectra at position 6 when the BLM is only at position 6 compared when the BLMs are in all positions.

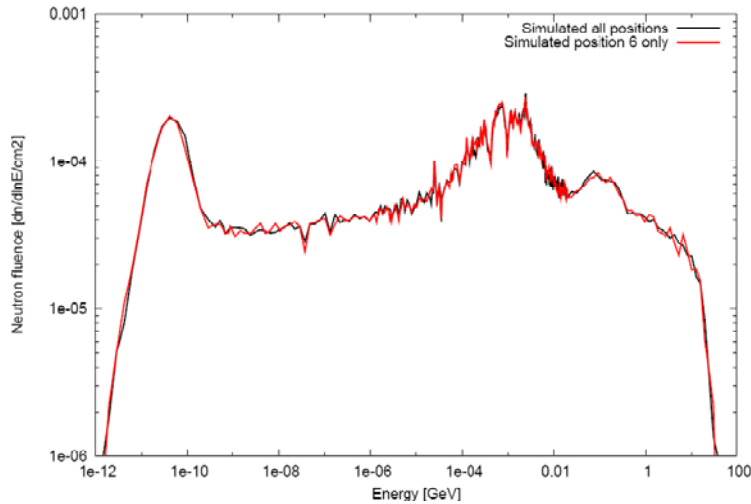


Figure 11: Neutron fluence in the BLM active volume located at position 6 for two scenarios: in black the BLMs are put in all positions, in red only one BLM is put at position 6.

In addition, in terms of energy deposition simulated in the BLM active volume, Table 8 compares the BLM signal as calculated by FLUKA and expressed in GeV per primary particle when the BLMs are put in all positions, and when one BLM is put successively at positions 1, 5 and 6. No significant differences are observed and for all other configurations only the combined simulation positions are used.

FLUKA simulation [GeV/p] - BLM horizontal without Cd - cables downstream										
	Simulated All positions	Error [%]	Simulated Position 1 only	Error [%]	Simulated Position 5 only	Error [%]	Simulated Position 6 only	Error [%]	Ratio One position/All	Error [%]
Position 1	1.68E-07	3.0	1.18E-07	5.5					0.89	8.5
Position 5	1.38E-05	0.6			1.31E-05	1.5			0.95	2.1
Position 6	2.89E-05	0.6					2.89E-05	1.7	1.00	2.3

Table 8: Comparison of the energy deposition as calculated by FLUKA in the BLM active volume at three positions.

The signal given by the BLM comes from the volume between the electrodes which is filled with Nitrogen. This volume is divided into two regions: the sensitive volume in between the electrodes and the outer layer around the electrodes. The electrical field collecting the charges, which results in the detector signal, is strongest between the electrodes and extends in radial direction for about 1/3 of the electrode spacing. Therefore the collection probability is significantly higher for a charged particle produced inside the sensitive volume than produced outside [9]. To evaluate a possible influence of the latter and differentiate the contribution of both volumes, two separate regions were defined in the FLUKA input file with Nitrogen gas set to the correct pressure as filling material for both of them.

The FLUKA results for the three BLM prototypes are presented in Table 9. FLUKA gives the results in GeV per primary particle. The ‘w’ conversion factor [10] gives for Nitrogen an average energy necessary to produce an electron-ion pair which is equal to 34.8 ± 0.2 eV. This factor together with the PIC calibration is used to convert the simulation results in values expressed as nC per PIC. The ‘w’ factor is a function of the gas, the type of radiation and its energy. However, in the effective energy range and for the main contributing particle types, it does not show a strong dependence, hence, can be approximated in most cases by a constant value [10].

The two last columns give the relative difference of the BLM signal between the cases with and without Cd, and the cases with and without a gap (representing the required spacing for the connection cables). For additional illustration, the last rows present for the 6 positions the relative difference in terms of signal between the horizontal BLM with the cables downstream and the horizontal BLM with the cables upstream.

No significant difference is observed between the prototypes 2 and 3, *i.e.*, by opening the Cd with a small gap of 2cm of diameter for the cable passages. The difference in this case ranges from 0.2% to 10% for the position 1, more sensitive to the thermal neutrons.

Around 5% of difference is observed between the cases with and without Cd, which is not significant. This is consistent with the measurements as presented in the first part of this report.

BLM orientation	Positions	FLUKA Simulation															
		BLM without Cd				BLM with Cd				BLM with Cd + gap				Relative difference Cd / no Cd [%]		Relative difference gap / no gap [%]	
		Outer layer		Sensitive volume		Outer layer		Sensitive volume		Outer layer		Sensitive volume		Out. Lay.	Sens. Vol.	Out. Lay.	Sens. Vol.
		[nC/PIC]	Error [%]	[nC/PIC]	Error [%]	[nC/PIC]	Error [%]	[nC/PIC]	Error [%]	[nC/PIC]	Error [%]	[nC/PIC]	Error [%]				
Horizontal cables downstream	1	3.02E-05	5.18	4.82E-05	4.23	2.94E-05	7.44	4.99E-05	3.95	3.17E-05	8.61	5.51E-05	8.78	2.8	-3.4	-7.9	-10.5
	2	9.50E-05	4.21	1.42E-04	2.84	8.51E-05	4.84	1.38E-04	5.14	8.35E-05	3.35	1.49E-04	6.06	10.4	3.0	1.8	-8.2
	3	4.62E-04	1.09	7.39E-04	1.14	4.57E-04	1.36	7.14E-04	1.54	4.61E-04	2.01	7.13E-04	3.10	1.1	3.3	-1.0	0.2
	4	5.40E-04	1.02	9.60E-04	0.75	5.13E-04	1.28	9.12E-04	0.97	5.29E-04	2.31	9.07E-04	1.69	5.0	5.0	-3.2	0.5
	5	8.57E-04	1.23	1.42E-03	0.59	8.56E-04	0.84	1.47E-03	0.94	8.48E-04	1.11	1.44E-03	0.87	0.1	-3.5	1.0	2.2
	6	1.81E-03	0.71	2.98E-03	0.55	1.98E-03	0.85	3.31E-03	0.60	1.95E-03	1.22	3.30E-03	0.86	-9.3	-11.2	1.5	0.5
Horizontal cables upstream	1	3.10E-05	5.70	4.86E-05	3.98	3.19E-05	5.87	4.97E-05	4.99	2.44E-05	8.73	4.42E-05	6.30	-2.9	-2.4	23.5	11.2
	2	7.95E-05	6.75	1.40E-04	3.91	8.78E-05	5.28	1.45E-04	2.58	8.13E-05	12.20	1.32E-04	4.30	-10.4	-3.4	7.4	9.0
	3	4.23E-04	1.28	7.35E-04	1.39	3.97E-04	2.13	6.91E-04	4.82	4.02E-04	5.57	7.28E-04	2.86	6.2	5.9	-1.2	-5.3
	4	5.21E-04	0.75	9.70E-04	0.99	4.97E-04	0.94	9.16E-04	0.77	5.11E-04	1.44	9.03E-04	1.32	4.6	5.6	-2.8	1.4
	5	8.67E-04	0.94	1.37E-03	0.73	8.76E-04	0.72	1.43E-03	0.95	8.74E-04	1.46	1.45E-03	1.86	-1.0	-4.4	0.2	-1.2
	6	1.80E-03	0.98	2.85E-03	0.74	1.93E-03	0.63	3.12E-03	0.75	1.93E-03	1.05	3.18E-03	1.01	-7.5	-9.6	0.2	-1.8
Vertical cables down	1	3.33E-05	7.18	5.68E-05	3.83	3.60E-05	9.18	5.85E-05	4.90	3.61E-05	10.70	5.25E-05	7.90	-8.1	-2.9	-0.5	10.2
	2	8.23E-05	2.75	1.46E-04	4.29	8.41E-05	7.30	1.58E-04	4.49	8.05E-05	5.01	1.48E-04	5.70	-2.3	-7.7	4.3	5.9
	3	3.84E-04	1.27	6.83E-04	1.09	3.58E-04	1.57	6.53E-04	1.14	3.56E-04	1.75	6.35E-04	1.47	6.7	4.4	0.5	2.7
	4	5.44E-04	1.19	9.93E-04	1.13	5.30E-04	1.50	9.48E-04	1.05	5.25E-04	1.78	9.22E-04	1.48	2.5	4.6	0.9	2.7
	5	8.85E-04	0.92	1.49E-03	0.93	9.03E-04	0.86	1.58E-03	0.63	8.98E-04	1.18	1.57E-03	1.13	-2.0	-6.1	0.5	1.0
	6	1.06E-03	0.92	2.05E-03	0.67	1.17E-03	0.72	2.30E-03	0.47	1.17E-03	1.88	2.32E-03	1.39	-10.2	-12.4	-0.2	-0.7
Relative difference [%] Hori. down/up	1	2.4		0.7		7.8		-0.3		-30.0		-24.7					
	2	-19.5		-1.6		3.1		4.8		-2.8		-13.3					
	3	-9.2		-0.5		-15.1		-3.3		-14.9		2.1					
	4	-3.6		1.1		-3.3		0.5		-3.6		-0.5					
	5	1.1		-3.5		2.2		-2.7		3.1		0.7					
	6	-0.7		-4.6		-2.4		-6.0		-1.1		-3.6					

Table 9: FLUKA results showing the BLM signal expressed in nC/PIC.

A higher difference of 10% to 12% can be observed at position 6, where the high energy particles are more dominant.

Finally almost no difference is observed in the BLM signal following its orientation. Again this conclusion given by the FLUKA simulations is similar to the one coming from the measurements. A certain difference is observed for the BLM prototype 3 at positions 1 and 2 dominated by the low-energy neutrons entering the gap. As shown in Table 9 (last column) about 10% of difference is observed at position 1 due to the gap, whereas it has no effect at position 6 dominated by the high-energy particles and no more by the low-energy neutrons as shown in Table 13.

To compare directly the FLUKA values with the measurements presented in the first paragraph (see Tables 4 to 6), Tables 10 and 11 show the ratio between the simulation and the measurements, separately for the case without Cd and the case with Cd. To possibly take into account the contribution from the outer layer, as explained above, the ratios after adding 5% and 10% of the signal from the outer layer are also presented.

BLM orientation	Position	Ratio FLUKA/MEASUREMENTS					
		BLM without Cd					
		Sensitive Volume	Error [%]	+ 5% Outer layer	Error [%]	+ 10% Outer layer	Error [%]
Horizontal cables downstream	1	1.24	5.5	1.28	5.8	1.32	6.0
	2	1.07	3.2	1.11	3.5	1.14	3.7
	3	1.24	3.4	1.28	3.5	1.31	3.5
	4	1.02	1.4	1.05	1.4	1.08	1.5
	5	1.22	0.7	1.25	0.8	1.29	0.8
Horizontal cables upstream	1	0.94	4.6	0.97	4.9	1.00	5.2
	2	1.04	4.1	1.07	4.4	1.10	4.8
	3	1.11	1.5	1.14	1.6	1.17	1.6
	4	1.07	1.8	1.10	1.8	1.13	1.9
	5	1.21	0.8	1.24	0.9	1.28	0.9
	6	1.08	1.3	1.11	1.4	1.15	1.4
Vertical cables down	4	1.06	1.7	1.09	1.8	1.12	1.8
	5	1.22	1.6	1.26	1.7	1.29	1.7
	6	1.13	1.9	1.16	1.9	1.19	2.0

Table 10: Comparison between the simulations and the measurements for the BLM without Cd.

BLM orientation	Position	Ratio FLUKA/MEASUREMENTS					
		BLM with Cd					
		Sensitive Volume	Error [%]	+ 5% Outer layer	Error [%]	+ 10% Outer layer	Error [%]
Horizontal cables upstream	1	1.00	5.5	1.04	5.8	1.07	6.1
	2	1.12	2.7	1.16	2.9	1.19	3.2
	3	1.01	5.0	1.04	5.1	1.07	5.2

Table 11: Comparison between the simulations and the measurements for the BLM with Cd.

The FLUKA results show a good agreement with the measurements. The difference is equal to 22% for position 5 and inferior to 13% for the others positions. However a difference of 24% is observed for the positions 1 and 3 when the cables are in the downstream direction. In fact, these measurements were performed during the first day and a serious doubt about the positioning was considered. During a second series of measurements, with a more precised positioning, the difference decreases to 6% for position 1 and 11% for position 3, but this time with the cables in the upstream direction and not in the downstream direction because of time constraint as already explained.

Furthermore the difference of 22% for the position 5 can be partly explained by again the uncertainties during the positioning of the detector in the CERF target area where the alignment of downstream beam elements is not guaranteed. Others uncertainties have to be taken into account as well. These uncertainties may come from the calibration of the ionization chamber (PIC), the beam shape or the beam misalignment. Previous studies [2] [5] show that these uncertainties can bring a variation of the detector signal from 10% to 20% at the downstream positions.

To better understand the sensitive energy region of the detector and the most contributing particle types (e.g., when the Cd is put around or not, or the signal at various positions), the BLM response has been determined with FLUKA simulations for different particle types, and different angles of the incident beam, using the BLM model well described as presented in the Figure 10. The BLM response simulations were performed with FLUKA to update the existing response curves as presented in [9]. A detailed stand-alone BLM geometry as well as a source defined for various particle types and energies were taken into account for each simulation. The concerned particles are neutrons, protons, pions, muons, photons, electrons and positrons for an energy range from 1 MeV to 10 TeV, except for neutrons and photons calculations for which the energy starts at respectively 10^{-14} eV and 100 keV. For two consecutive orders of magnitude, nine equidistant energy values in logarithmic scale were considered, e.g., between 1 MeV and 10 MeV: 1.258, 1.584, 1.995, 2.511, 3.162, 3.981, 5.011, 6.309 and 7.943. For each particle and each energy the energy deposition in the BLM sensitive volume was calculated and using the w-factor [10] the FLUKA result was converted into charge production. Figures 12 and 13 show for all particles the response function for an incident beam at 0° for Figure 12 and 90° for Figure 13. For convenience the response function for an incident neutron beam is put in a separate graph.

It has to be noticed that an incident beam of 0° corresponds to the BLM in the horizontal position with the cables in the downstream direction, *i.e.* the beam hits first the sensitive volume of the detector and not the electronic part.

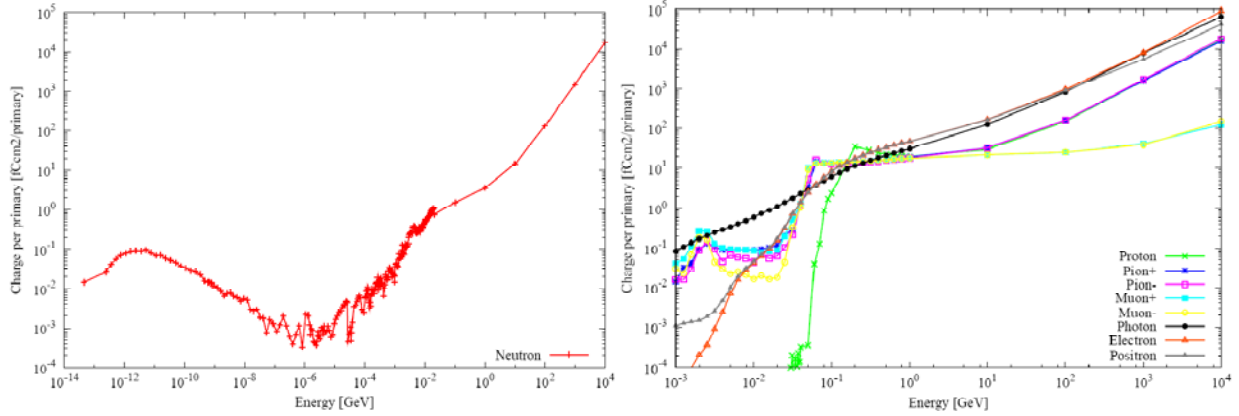


Figure 12: Response function expressed in $fC.cm^2/primary$ as a function of energy for a beam incident of 0° .

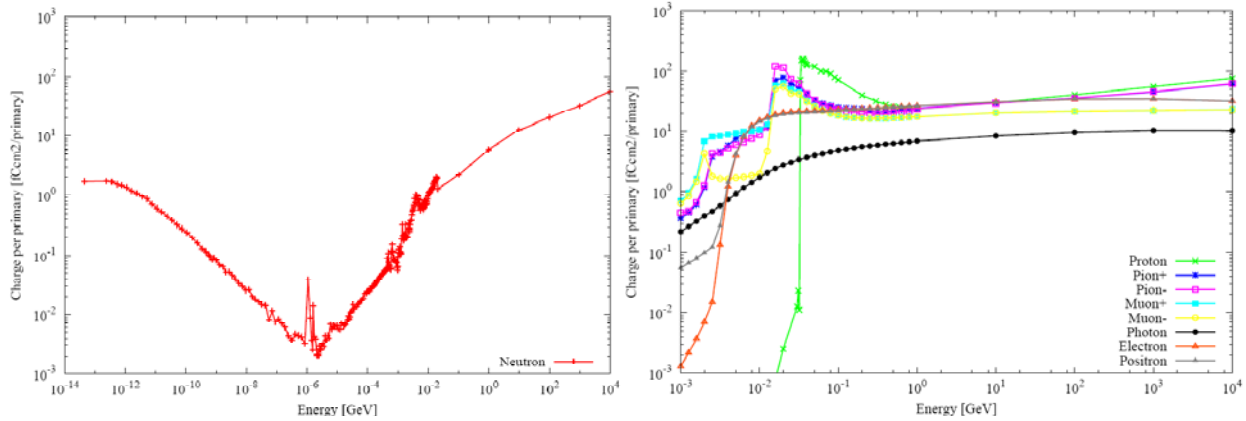


Figure 13: Response function expressed in $fC.cm^2/primary$ as a function of energy for a beam incident of 90° .

In addition, the energy spectra of the different particle types were simulated at each position, using an empty volume detector, thus representing the particle energy spectra entering the BLM chamber, as presented in Figure 3 for neutrons at all positions and Figures 5 and 6 for all particles at positions 1 and 6. The pre-calculated response functions were then folded with the particle spectra using an online routine in order to calculate the detector signal as a function of energy and particle type. Two cases were studied and compared in detail: the case without Cd around the empty volume detector, and the case with 1 mm of Cd, both for positions 1 and 6. Figure 14 shows the spectrum, the response function and the folding of the two for the neutrons at position 1.

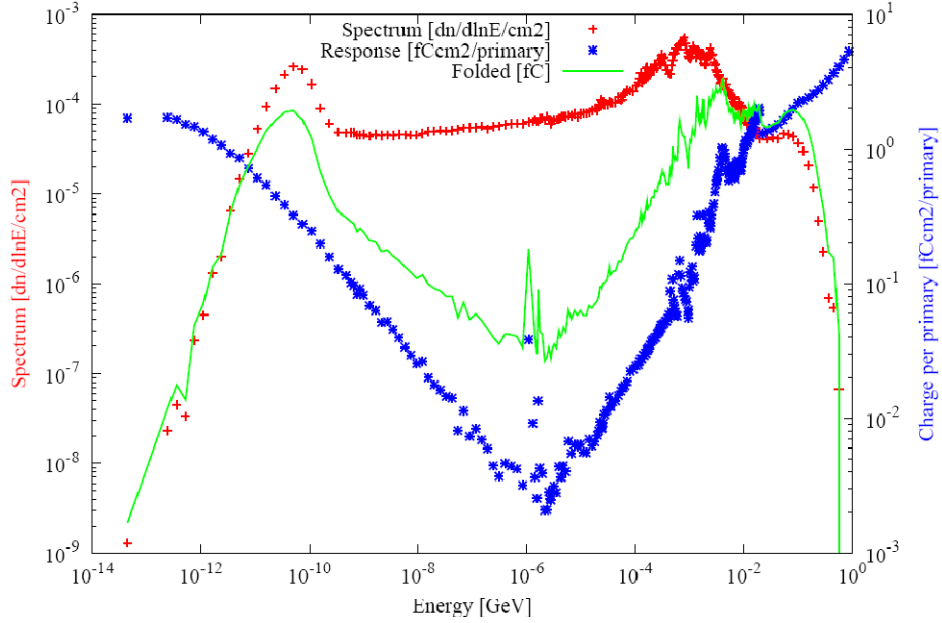


Figure 14: Spectrum, response function and expected signal (in arbitrary unit) for neutrons at 90° .

Furthermore, to compare the folding method with the direct scoring, Table 12 gives the energy deposition in the BLM active volume converted in charge obtained with both methods. A comparison is given for a response function at 90° w.r.t. the beam direction.

BLM signal [fC/primary] - BLM horizontal without Cd - cables downstream						
	Direct scoring	Error [%]	Folding method 90°	Error [%]	Ratio Folding 90° /Direct	Error [%]
Position 1	2.20E-03	4.2	2.70E-03	4.4	1.23	8.6
Position 3	3.30E-02	1.1	4.00E-02	1.8	1.21	2.9
Position 6	1.33E-01	0.6	1.05E-01	1.4	0.79	1.9

Table 12: BLM signal as calculated with FLUKA using 2 different methods, at 90° w.r.t. the beam direction.

Figures 15 and 16 show the signal of the main contributing particles as a function of energy in a horizontally placed detector using the response functions for 135° with respect to the beam direction corresponding to position 1 (see Figure 15) and respectively 0° for position 6 (see Figure 16). For convenience the neutron signal is put in a separate graph.

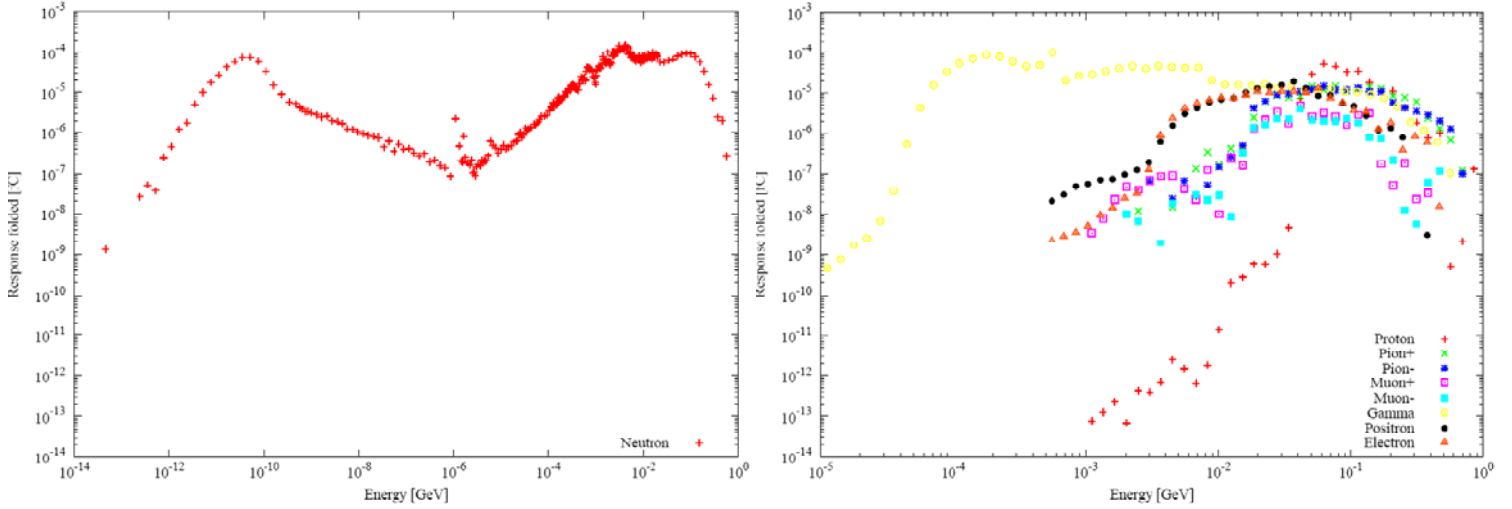


Figure 15: Signal of the main contributing particles as a function of energy in a horizontal BLM using a response function calculated for 135° w.r.t. the beam direction (position 1).

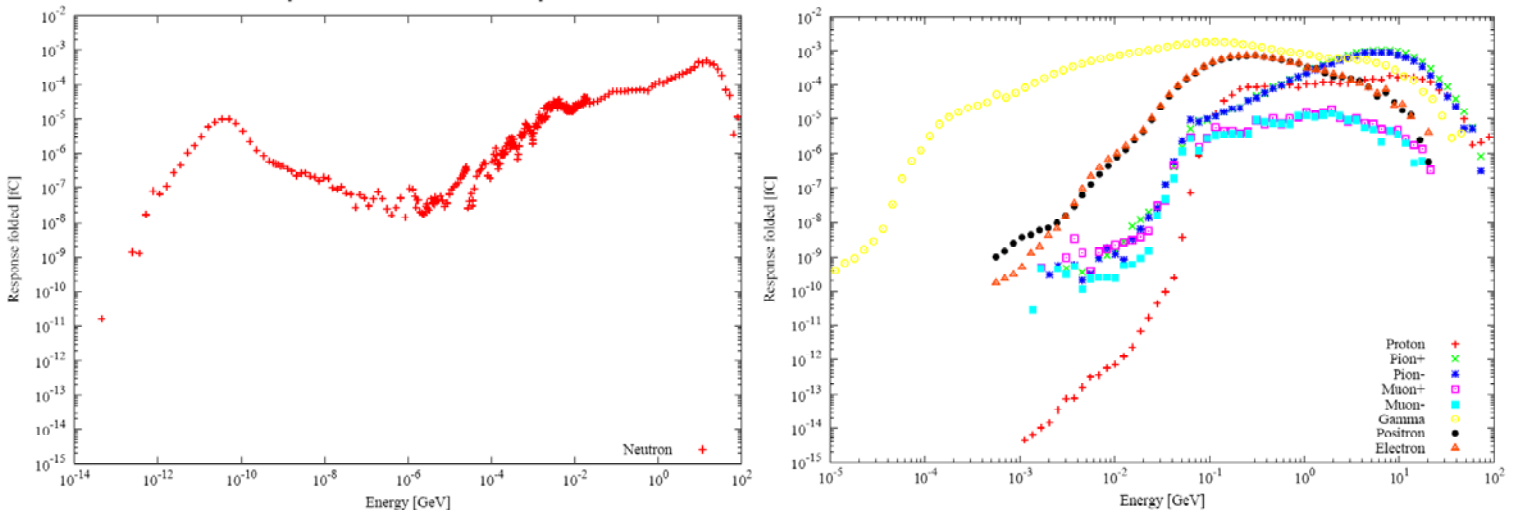


Figure 16: Signal of the main contributing particles as a function of energy in a horizontal BLM using a response function calculated for 0° w.r.t. the beam direction (position 6).

To visualize the BLM signal with the presence of the Cd foil, Figure 17 compares the neutron spectra at position 1 in the BLM with Cd and in the BLM without Cd. As one can see, there is no contribution of the thermal neutrons for the BLM surrounded by a Cd layer.

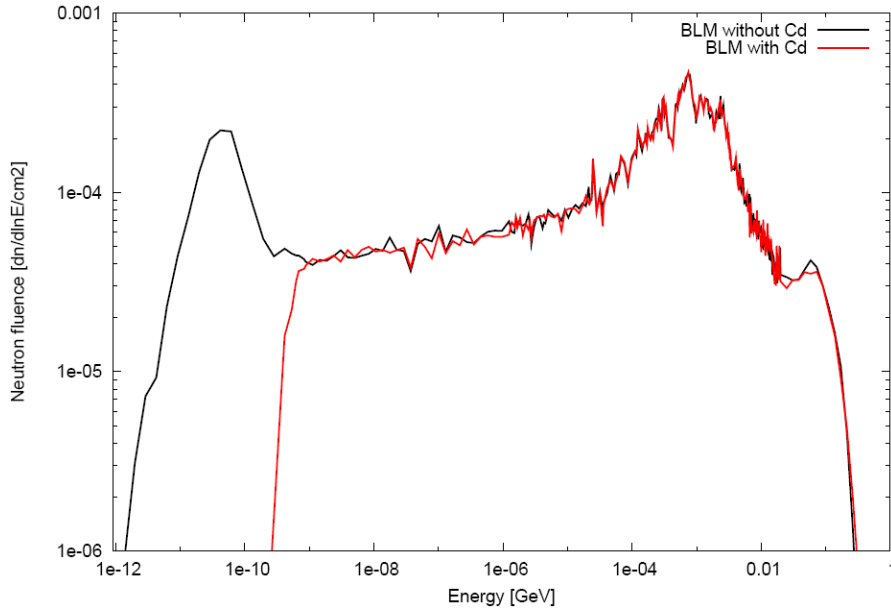


Figure 17: Comparison of neutron spectra in the BLM with cadmium and the BLM without cadmium.

However, the BLM signal remains almost the same for both cases, as shown in the Table 9. Assuming that the loss of the thermal neutrons contribution may be compensated by the photons coming from the Cd, the photons spectra entering a volume detector located at position 1 was simulated, first without Cd around this volume and then including a layer of 1 mm of Cd. The change in the photon spectra is illustrated in Figure 18 and shows a contribution of gammas higher by a factor 2 when the Cd is put around the volume detector in the energy range between 1 MeV and 10 MeV.

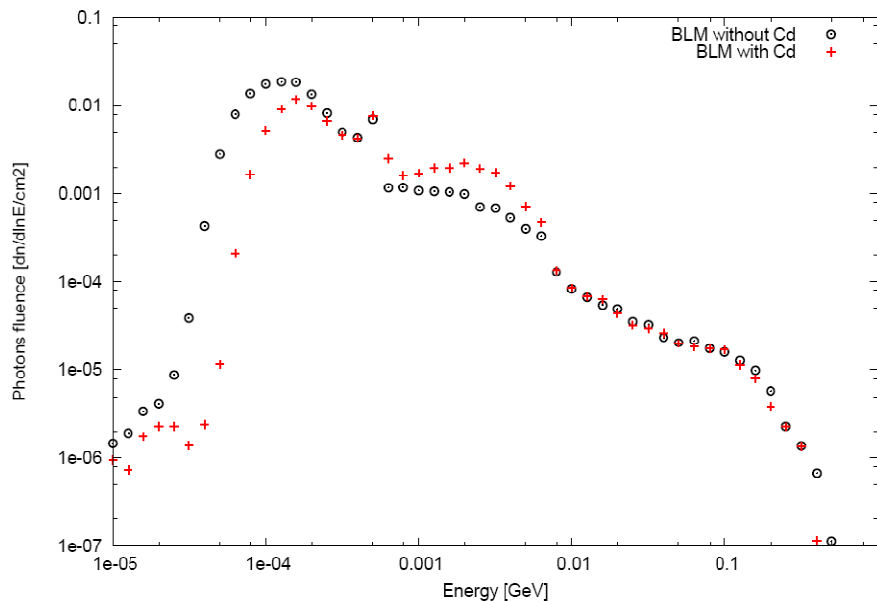


Figure 18: Comparison of photon spectra entering the BLM with Cd and the BLM without Cd.

In the same respect, Table 13 presents the contribution of the main particles expressed as percentage of the signal for the respective radiation fields at CERF. The results were obtained with the folding method assuming a BLM horizontally oriented with the cables downstream and a detector response with a beam incident of 90° for position 3, 135° for position 1 and 0° for position 6. The presented results show statistical uncertainties below 10%. Besides for neutrons at position 1 almost no difference is observed in terms of particles contribution between the signal of the BLM with Cd and the BLM without Cd for the positions 3 and 6. For position 1, the neutron contribution decreases with the Cd (cut for thermal neutrons). In terms of the total signal, as already observed by the measurements, the loss of 6% to 7% in the total neutron contribution is compensated by the gain of 10% in the photons contribution, when the Cd is put around the BLM. Almost no difference is noticed for the others particles contribution when both BLMs, with and without Cd, are put at position 1.

BLM configuration	Position	Particles contribution [%]											
		n				p	π^+	π^-	μ^+	μ^-	γ	e+	e-
		< 0.5 eV	0.5eV<n<20MeV	>20MeV	Total								
Horizontal cables downstream without Cd	1	6.2	10.7	6.3	23.3	9.3	5.7	5.4	1.1	0.9	44.0	5.5	4.9
	3	0.6	4.8	4.2	9.6	20.7	6.4	6.3	0.5	0.3	31.8	11.1	13.3
	6	0.03	0.1	1.5	1.6	3.9	14.9	12.3	0.3	0.2	44.0	11.2	11.5
Horizontal cables downstream with Cd	1	0.03	10.7	6.4	17.1	8.3	4.4	5.0	1.1	0.9	52.8	5.3	5.2
	3	0.003	5.0	4.3	9.3	20.5	6.4	6.5	0.5	0.3	32.9	10.9	12.5
	6	0.0001	0.1	1.6	1.7	4.3	14.7	12.5	0.3	0.2	42.4	11.9	12.2

Table 13: Main contributing particles for the respective radiation field at CERF. The BLM with Cd is compared with the BLM without Cd.

As shown in Table 13, the main contributing particles at position 1 are photons, neutrons and protons, whereas the BLM signal at position 6 is mainly due to the photons, pions, electrons and positrons. Figures 19 to 20 show the spectra and the folded response of these main contributing particles in a horizontal BLM with the cables downstream located at position 1 for Figure 19 and position 6 for Figure 20. Both cases are compared, one with Cd and one without Cd.

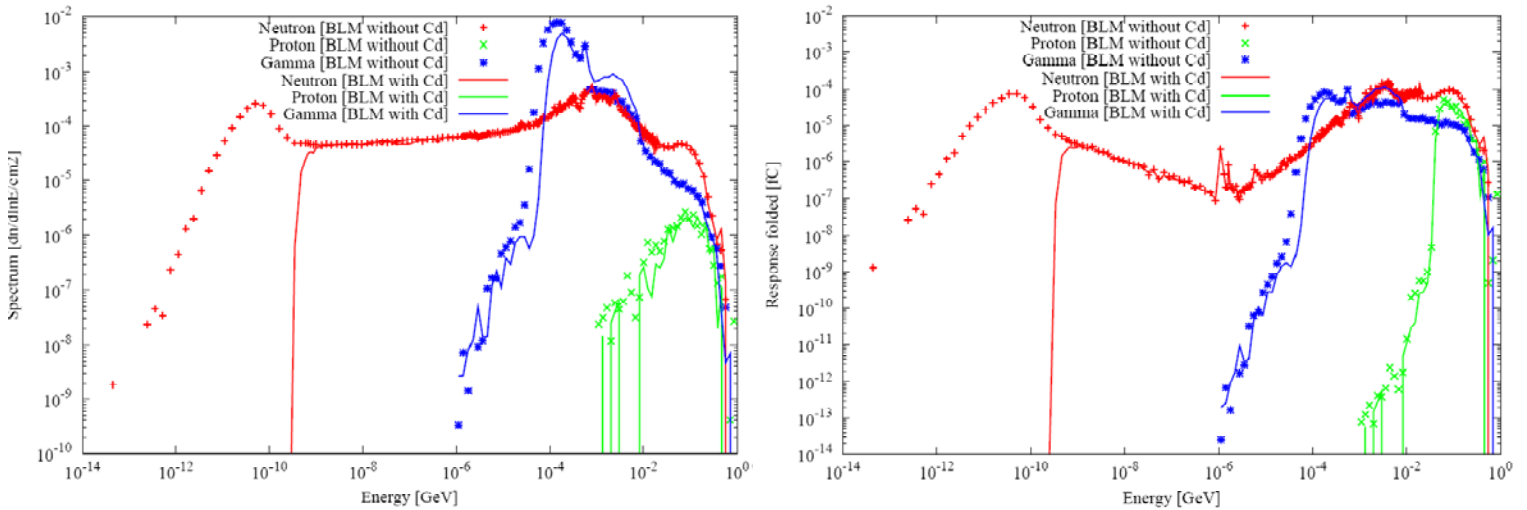


Figure 19: Spectra (at left) and signal (at right) of the main contributing particles at position 1 for both cases with and without Cd.

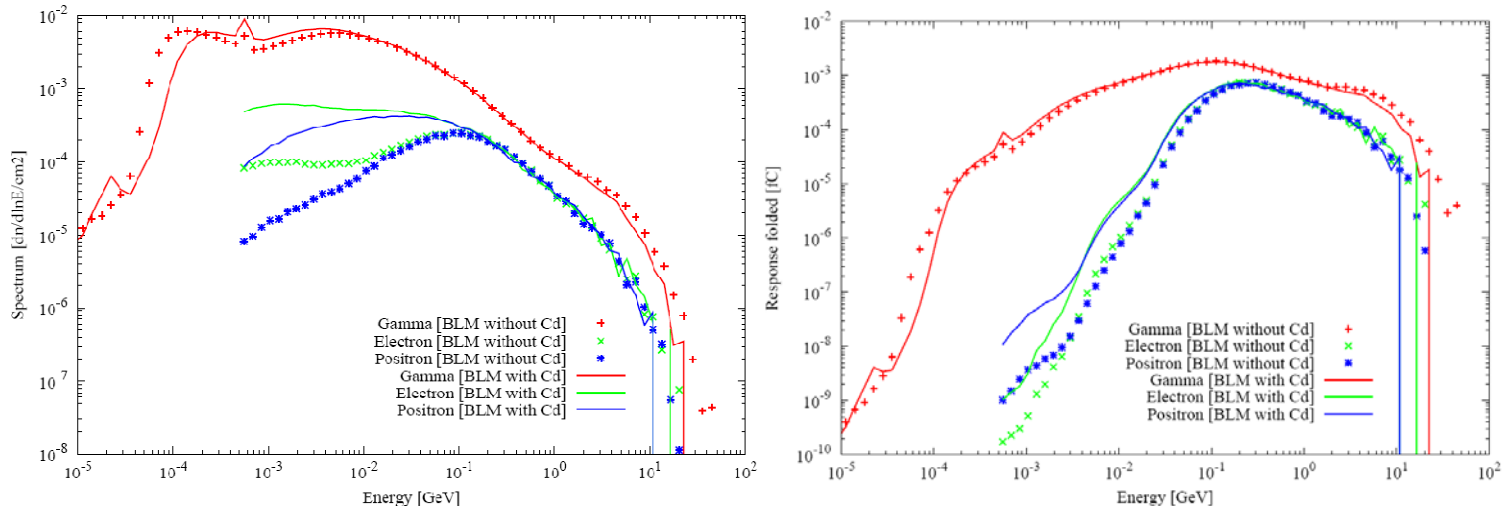


Figure 20: Spectra (at left) and signal (at right) of the main contributing particles at position 6 for both cases with and without Cd.

4. Conclusion

The CERF facility at CERN is used as a reference for testing, inter-comparing and calibrating passive and active instrument. In May 2009, the SPS provided a positively charged hadrons beam during few days in order to perform measurements with several devices. This report presents those performed with the Beam Loss Monitor (BLM), which is used to detect beam losses in the LHC dispersion suppressor, arcs, inner triplets as well as the beam-cleaning insertions. The main objective of this year's measurements was to test the sensitivity of the BLM signal to the radiation field by using a Cd layer wrapped around the detector, as well as by changing the orientation of the detector following the beam direction. In parallel the FLUKA Monte Carlo code was used to evaluate the BLM response in terms of energy deposition and particles spectra. The measurements results as well as the FLUKA calculations are presented in this paper.

The measurements were performed at different locations around the CERF target, and the BLMs were put either with the cables upstream or with the cables downstream. The difference in the BLM signal was not significant, around 10% depending on the location of the detector around the target, at all positions well reproduced by the corresponding FLUKA calculations. This confirms that the horizontal chamber orientation is not important when comparing BLM measurements with simulations at the LHC (at typical locations next to warm and cold magnets).

Verifying the contribution of low-energy neutrons to the BLM signal both measurements and simulations showed no significant difference in the BLM signal after wrapping it with 1 mm of Cd. This observed difference is in the order of 3% to 4%. Furthermore the contribution of low-energy neutrons to the BLM signal is very small. Without Cd around the BLM, this contribution is equal to 6%. This is an important conclusion, as in the existing LHC simulations an important uncertainty has to be taken into account when estimating thermal neutron fluences. The latter are

dominated by the surrounding material (insulation, water content of concrete, installed equipment) which are not (and cannot be) always included in all details in the simulations.

The BLM measurements are directly compared with the FLUKA values for most of the positions around the target. This comparison shows a good agreement and it is also the case for the measurements performed with the Cd. Without Cd, the difference is equal to 22% for position 5 (downstream of the target) and inferior to 13% for the others positions. With Cd the difference is inferior to 12%. This difference of 22% for position 5 can be partly explained by positioning uncertainties especially in the most downstream part where the alignment of the beam-line is not guaranteed. Indeed in case of a misalignment of the beam-line, the latter is worst at the downstream locations than at the target position. Further uncertainties concern the calibration of the ionization chamber (PIC), the beam shape and alignment. The downstream locations showing a strong gradient, these uncertainties can strongly modify the measured signal (as shown in [2] and Figure 4).

This final study focused on the signal dependencies as a function of detector orientation, a possible low-energy neutron contribution and the analysis of which particles contribute most at what energies. Therefore, in order to analyze in detail the observed BLM signal and study its dependency on particle energy and type additional FLUKA simulations were performed to get the contribution of the main particles to the BLM signal, and to study the difference observed when the Cd is put around the BLM not only based on integral values, but as a function of particle type and energy. This required the calculation of a full set of BLM response functions (various particle types and energies). These response curves can then be folded with the particle energy spectra at the various locations, thus allowing for a detailed study of the BLM signal as a function of particle type and energy.

For the case where the chamber is wrapped in cadmium a loss of 6% to 7% in the total neutron contribution is observed which is actually compensated by the gain of 8% to 9% in the photons contribution. At the upstream position, the photons, neutrons and protons are more dominant with almost 53% of the BLM signal coming from photons, 17% from neutrons and 8% from protons. At the downstream position, BLM signal is mainly due to the photons, pions, positrons and electrons with 42% coming from the photons, 14% from the positive pions, 12% from the negative pions, 12% from the electrons and the positrons.

To summarize, this study aimed at a detailed comparison between the measured BLM signal at LHC representative locations, as well as a respective analysis in terms of contributing particle type and energy. This was motivated by the fact that the BLM chambers are used at various LHC locations, with different particle energy spectra, thus requiring a detailed analysis when measured BLM signals are compared with respective Monte-Carlo simulations during early LHC operation. It could be shown that the contribution of thermal neutrons to the total signal remains minor. After wrapping the BLM with 1 mm of Cd to cut the thermal neutron contribution, the total signal is partly compensated by the production of secondary photons, thus remains the same, which shows again a non-important contribution from the thermal neutrons. Since the CERF spectra at the respective BLM locations are comparable with those at the LHC [2] (see also Figure 3), the contribution of thermal neutrons to the total signal remains minor for the expected LHC locations. This is important as the prediction of low-energy neutron fluences

based on simulations has a significant uncertainty due to the materials used (e.g., insulation material, water content of concrete), as well as the installed equipment (racks, electronics, etc.). In addition, the sensitivity of the observed signal as a function of chamber orientation has been shown to be minor, again important when early BLM measurements are compared with previously performed LHC simulations and where the orientation of the chamber was not considered in the past. The detailed analysis of particle energy spectra, the BLM detector response, the main contributing particles to the chamber signal and the comparison between measurements and simulations allow for a complete study of the BLM detector.

5. Acknowledgements

The authors would like to thank the DG/SCR (RP) group for their help and support in setting-up and providing the CERF facility. Christian Theis, Eduard Feldbaumer and Helmut Vincke for their help with the calibration and installation of the PIC chamber, as well as Paola Sala for providing the original detailed FLUKA input of the BLM chamber.

6. References

- [1] A. Mitaroff, M. Silari, The CERN-EU high-energy Reference Field (CERF) facility for dosimetry at commercial flight altitudes and in space, *Radiation Protection Dosimetry* 102, p. 7-22 (2002).
- [2] L. Sarchiapone, M. Brugger, B. Dehning, D. Kramer, M. Stockner, V. Vlachoudis, FLUKA Monte Carlo simulations and benchmark measurements for the LHC beam loss monitors, *Nuclear Instruments and Methods in Physics Research A* 581 (2007) 511-516, www.sciencedirect.com, 7 August 2007.
- [3] A. Fasso`, A. Ferrari, J. Ranft, and P.R. Sala, *FLUKA: a multi-particle transport code*, CERN- 2005-10 (2005), INFN/TC_05/11, SLAC-R-773.
- [4] G. Battistoni, S. Muraro, P.R. Sala, F. Cerutti, A. Ferrari, S. Roesler, A. Fasso`, J. Ranft, "*The FLUKA code: Description and benchmarking*", Proceedings of the Hadronic Shower Simulation Workshop 2006, Fermilab 6--8 September 2006, M. Albrow, R. Raja eds., AIP Conference Proceeding 896, 31-49, (2007)
- [5] H. Vincke, S. Mayer, I. Efthymiopoulos, A. Fabich, D. Forkel-Wirth, M. J. Müller, C. Theis, Accurate PIC calibration by the use of a coincidence of two scintillators, Technical Note CERN-SC-2004-090-RP-TN, EDMS 536144.
- [6] H. Vincke, N. Aguilar, D. Forkel-Wirth, M. Pangallo, D. Perrin, M. Renou and C. Theis, Measurements and Simulations of the PMI Chamber Response to the Radiation Field inside the CERF Target Area, Technical Note CERN-SC-2004-025-RP-TN, EDMS 457017 .

- [7] K. Shibata et al. Japanese Evaluated Nuclear Data Library Version 3 Revision-3: JENDL-3.3. *Journal of Nuclear Science and Technology*, 39(11), (2002) 1125-1136.
- [8] Ferrari, A ; Guglielmi, A M ; Lorenzo-Sentis, M ; Roesler, S ; Sala, P R ; Sarchiapone, L, An updated Monte Carlo calculation of the CNGS neutrino beam, CERN-AB-Note-2006-038 2006.
- [9] M. Stockner, Beam Loss Calibration Studies for High Energy Proton Accelerators, CERN-THESIS-2008-099, Vienna, October 2007, CDS 1144077.
- [10] Seventh International Commission on Radiation Units and Measurements, Average Energy Required to Produce an Ion Pair, ICRU Report 31, Washington, DC, 1979.